IEEE Access
Multidisciplinary | Rapid Review | Open Access Journal

Received 19 December 2023, accepted 26 January 2024, date of publication 22 February 2024, date of current version 11 March 2024.

Digital Object Identifier 10.1109/ACCESS.2024.3368912

RESEARCH ARTICLE

Miniaturized Continuous-Wave Terahertz Spectrometer With 3.6 THz Bandwidth Enabled by Photonic Integration and Microelectronics

SIMON NELLEN[1], LAURI SCHWENSON[1], LARS LIEBERMEISTER[1], MILAN DEUMER[1], SEBASTIAN LAUCK[1], MARTIN SCHELL[1,2], (Member, IEEE), AND ROBERT B. KOHLHAAS[1]

[1]Fraunhofer Institute for Telecommunications, Heinrich Hertz Institute, 10587 Berlin, Germany
[2]Institut für Festkörperphysik, Technische Universität Berlin, 10623 Berlin, Germany

Corresponding author: Simon Nellen (simon.nellen@hhi.fraunhofer.de)

ABSTRACT Broadband terahertz spectroscopy is a valuable analytical tool in science and a promising technology for industrial non-destructive, non-contact testing, e.g. thickness measurements of thin dielectric layers. Optoelectronic conversion using photomixers is a widespread approach for coherent terahertz spectroscopy. State-of-the-art spectrometers consist of discrete, fiber-based components, leading to complex and costly setups. In cost-sensitive applications, this prevents the use of these spectrometers. We developed a terahertz spectrometer based on a dedicated photonic integrated circuit and commercial electronic integrated circuits to overcome these limitations. The photonic subsystem can be connected to commercial tunable lasers and provides the optical signal processing to drive the photoconductive antennas. The electronic subsystem includes the required drivers, analog signal processing, and data acquisition. Combined, the system measures $10 \times 16 \times 7.5$ cm^3 only. We compare both subsystems individually and as a whole to state-of-the-art lab equipment in terms of spectral performance and measurement speed. Due to the flexibility in measurement modes, the integrated system can be adapted to specific measurement tasks, e.g. 2.8 THz-wide spectra within 0.5 s for high-speed, or 3.6 THz bandwidth with >80 dB dynamic range in less than 3 minutes for high-precision. This is the first realization of a terahertz spectrometer based on photonic and electronic integration rivaling state-of-the-art and non-integrated commercial spectrometers. This approach paves the way for compact and economic terahertz systems, providing access to terahertz technology for cost-sensitive sectors in research and industry.

INDEX TERMS Terahertz, terahertz spectroscopy, frequency domain, photomixing, optoelectronic, photonic integration, photonic integrated circuit, electronic circuit design, miniaturization.

I. INTRODUCTION

Terahertz spectroscopy based on optoelectronic techniques is a well-established scientific tool and a promising technology for applications related to material analysis and non-destructive testing [1], [2], [3]. To date, mainly time-domain spectroscopy (TDS) is used when high bandwidth and high measuring rates are required, e.g. for layer thickness determination or defect detection [4], [5], [6], [7]. A competitive approach is continuous-wave (cw) terahertz spectroscopy by photomixing [8], [9], [10], [11], [12], [13]. Using precise tunable lasers and state-of-the-art photoconductive antennas, the bandwidth of cw terahertz spectrometers spans from below 100 GHz up to 4.5 THz with a resolution below 7 MHz [1], [14], [15], [16].

The associate editor coordinating the review of this manuscript and approving it for publication was Derek Abbott.

© 2024 The Authors. This work is licensed under a Creative Commons Attribution-NonCommercial-NoDerivatives 4.0 License.
For more information, see https://creativecommons.org/licenses/by-nc-nd/4.0/

Employing mature telecom lasers, this approach also enables measurement rates of up to 200 spectra per second [17].

Such a cw terahertz system offers higher frequency resolution and accuracy compared to TDS [13]. While TDS provides the highest resolution for extremely thin layers, the cw terahertz system is also capable of achieving similar results. Previous studies have demonstrated the ability of the cw system to resolve layers as thin as a few tens of micrometers, thereby meeting the requirements of numerous industrial applications [11].

In contrast to TDS systems, which rely on short optical pulses in the femtosecond range and often variable optical delay lines, all parts of a cw terahertz system exist as photonic integrated components. Thus, cw terahertz technology offers great potential for photonic integration. That makes this approach suited to address two major criteria for widespread employment: small size and scalable costs.

In previous work on on-chip photonic integrated cw terahertz devices, mainly the optical signal generation and the optoelectronic conversion have been addressed [18], [19], [20], [21], [22], [23], [24], [25]. Besides that, based on fiber-optical components, a terahertz spectrometer with enhanced signal acquisition has been demonstrated using a polarization selective phase modulator [26], [27]. Although this approach enabled two orders of magnitude faster frequency scans compared to the state-of-the-art, the amount of required fiber components resulted in high insertion losses and non-scalable footprint and costs.

In this work, we present a photonic integrated circuit (PIC) on an 18 mm^2 chip that provides similar optical signal processing to enable instantaneous coherent terahertz detection. Therefore, a phase modulation unit (PMU) is realized with optical phase modulators and optical amplifiers based on InP technology. In addition, we demonstrate a miniaturized electronic system to drive the developed PMU PIC, acquire the detector signal, and process the measured data to spectrally resolved phase and amplitude data. Since the integrated system is fiber-pigtailed, external tunable lasers and photoconductive antennas (PCAs) can be attached to access the full bandwidth of state-of-the-art cw terahertz spectroscopy.

In the following section II, we will first discuss the principle of coherent terahertz measurements using active optical phase modulation. In section III, the photonic integrated PMU is presented and evaluated. Finally, the miniaturized electronics for control and acquisition is described and evaluated in section IV.

II. COHERENT SPECTROSCOPY USING ACTIVE PHASE MODULATION

Terahertz generation and detection by photomixing rely on creating a photonic local oscillator (PLO) by superposition of two optical laser signals. Since each laser signal has a certain amplitude A_i, angular frequency $\omega_i = 2\pi f_i$, and phase φ_i, the power of the superposed lasers P_{beat} is given by

$$P_{beat} \propto E_{beat}^2 = |E_1 + E_2|^2 = |A_1 \cdot \cos(\omega_1 t + \varphi_1) + A_2 \cdot cos(\omega_2 t + \varphi_2)|^2 . \quad (1)$$

At the emitter (Tx), an ultrafast photodiode converts the envelope of the optical signal into an electrical signal that is radiated from an attached antenna. Thus, only the envelope of the optical beat signal contributes to the emitted terahertz signal [8], [17]:

$$E_{THz} \propto A_{THz} \cdot \cos(\Omega_{THz} t + \Phi_{THz}) \quad (2)$$

The electric field of the emitted terahertz radiation E_{THz} has a certain amplitude A_{THz} that oscillates with the difference frequency of the two lasers $\Omega_{THz} = |\omega_1 - \omega_2|$ and has the phase $\Phi_{THz} = \varphi_1 - \varphi_2$.

At the receiving PCA (Rx), the terahertz signal is down-converted using the PLO, i.e. the optical beat signal. The PLO modulates the conductance of the photoconductive gap of the PCA. In analogy to (1) and (2), the local oscillator at the receiver can be described by

$$PLO_{Rx} \propto A_{PLO} \cdot \cos(\Omega_{PLO} t + \Phi_{PLO}) . \quad (3)$$

When the electric field of the incoming terahertz signal applies to the receiving PCA, a detector current is generated:

$$I_{Rx} \propto A_{THz} \cdot A_{PLO} \cdot \cos((\Omega_{THz} - \Omega_{PLO}) t + (\Phi_{THz} - \Phi_{PLO})) \quad (4)$$

Note that for homodyne spectroscopy the same pair of lasers is used to drive Tx and Rx. Thus, the frequency of the emitted signal is the same as the PLO for down-conversion ($\Omega_{THz} = \Omega_{PLO}$), but due to the path difference, the phase of the terahertz signal and the PLO are different ($\Phi_{THz} \neq \Phi_{PLO}$). Thus, the current measured at the PCA Rx is DC in case of homodyne detection:

$$I_{Rx,DC} \propto A_{THz} \cdot A_{PLO} \cdot \cos(\Phi_{THz} - \Phi_{PLO}) \quad (5)$$

Also due to the path difference for Tx and Rx, the phase difference depends on the frequency. Thus, the Rx current exhibits a sinusoidal envelope when the frequency is tuned for spectral measurement. In a post-processing step, the original spectrum can be recovered by calculation of the Hilbert transform.

To avoid this frequency-dependent envelope and to provide amplitude and phase information instantaneously at any frequency point of the terahertz spectrum, active phase modulation is introduced. Therefore, Φ_{THz} or Φ_{PLO} are modulated with ω_{mod} to generate a time-dependent detector current. For example, when the PLO at the receiver is modulated, the resulting detector current is

$$I_{Rx,mod}(t) \propto A_{THz} \cdot A_{PLO} \cdot \cos(\Phi_{THz} - \Phi_{PLO}(t)) = A_{THz} \cdot A_{PLO} \cdot \cos(\omega_{mod} t + (\Phi_{THz} - \Phi_{PLO})) . \quad (6)$$

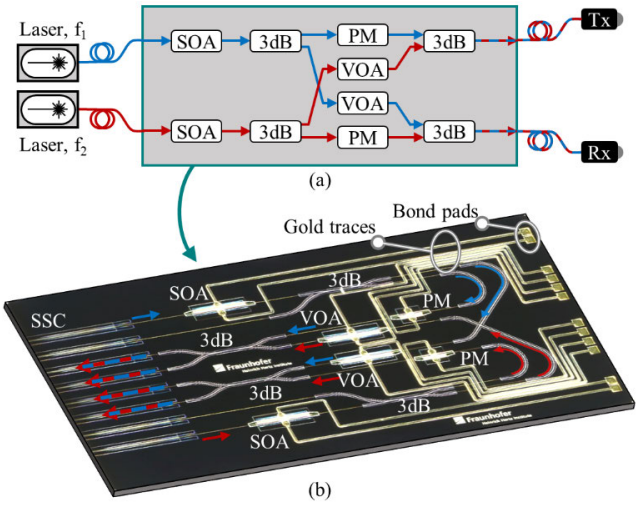

FIGURE 1. Schematic (a) and micrograph (b) of the photonic integrated phase modulation unit i-PMU with two optical amplifiers (SOA), two variable optical attenuators (VOA), four 3 dB couplers (3dB), and two phase modulators (PM) on the chip. Waveguides with spot size converters (SSC) are used to couple the optical signals from the fiber into the chip and vice versa.

The frequency of the active modulation ω_{mod} allows for lock-in detection to directly extract amplitude and phase of the detected signal.

III. PHOTONIC INTEGRATED PHASE MODULATION UNIT

A. DESIGN AND FABRICATION OF THE PMU

In order to detect and sample amplitude and phase of a terahertz signal for each frequency step, coherent cw terahertz spectrometers must employ a phase modulation unit (PMU) to shift the phase of the optical beat signal. Thereby, a sinusoidal detector current according to (6) is acquired and used for lock-in detection.

Active PMUs can be divided into two categories: i) mechanisms that delay the optical beat signal for the emitter or receiver arm, or ii) units that shift the phase of the optical beat signal by adjusting the phase of only one of the two laser tones before superposition into the beat note. A widespread example for i) are mechanical fiber-stretchers [28]. Concept ii) has been demonstrated with wavelength-selective optical phase modulators [26], [27]. Although the second concept is suitable for high-speed spectrometers, so far it has only been realized based on complex and costly discrete fiber components. Based on concept ii), we present a single photonic integrated circuit that serves as the PMU using Fraunhofer HHI's InP foundry platform [29], [30]. This *i*ntegrated *PMU* is referred to as *i-PMU* in the following.

Phase modulators (PM) change the refractive index of the guiding medium to delay the optical phase. The induced phase shift can be described by:

$$\Delta\Phi_{\mathrm{PM}} = L \cdot \omega \cdot \frac{\Delta n}{c_0} \tag{7}$$

c_0 is the speed of light and $\omega = 2\pi \cdot f$ is the angular frequency. Accordingly, the phase tuning is limited by the maximum possible change of the refractive index Δn and the length L of the modulator. In InP, the change of refractive index is limited to a magnitude of $\Delta n \approx 3 \cdot 10^{-3}$ within the optical c-band [30]. Thus, for a 2π shift of the optical beat signal $f = 1$ THz a modulator length of $L = 0.1$ m is required. Since that is magnitudes higher than the available chip size, we shift the phase of only one of the optical laser lines, which leads to a phase shift of the optical beat signal after superposition with the second optical line. In that way, a modulator length of $L \approx 522\ \mu$m is sufficient for a 2π shift with laser lines in the optical c-band.

Fig. 1 (a) shows the scheme of the photonic integrated circuit that provides a phase-modulated beat signal to emitter (Tx) and receiver (Rx), respectively: Two external lasers with the dedicated frequency spacing $f_{\mathrm{THz}} = |f_1 - f_2|$ are fed into the phase modulation unit. Semiconductor optical amplifiers (SOAs) allow to pre-compensate the losses of the following waveguide network. After amplification, a 3 dB splitter feeds a portion of the optical light into a phase modulator (PM) and a variable optical attenuator (VOA), respectively. The VOAs are used to emulate the insertion losses of the phase shifters and level the optical power in both paths. Finally, 3 dB couplers combine the phase-shifted signal from one laser with the fixed-phase signal from the other laser. In that way, Tx and Rx output ports provide a beat signal, which can be modulated in phase independently. Note that usually only Tx or Rx are modulated for coherent spectroscopy.

For the implementation on the generic InP platform, the design is folded in order to have input and output ports on the same facet. The resulting 6 mm × 3 mm sized integrated phase modulation unit is called *i-PMU*. Fig. 1 (b) shows a micrograph of the chip with the active building blocks labeled. The 3 dB splitters and combiners are realized as 2 × 2 multimode interferometers (MMIs). The phase modulators are based on current injection. Spot size converters (SSCs) are located at the left facet of the chip to match the mode field diameter for optical coupling to a fiber of all input and output ports. For electrical driving of the *i-PMU*, gold-plated bias pads are located at the right edge of the chip to contact all active components. To ease the handling of the *i-PMU* in a spectroscopic setup, the chip was packaged into a robust metal housing. Optical coupling to a fiber array allows using the *i-PMU* module in a fiber-coupled cw terahertz spectrometer. Multi-pin sockets for DC connection and coaxial connectors for the electrical modulation signal ensure compatibility with commercial lab equipment. For thermal stabilization, i.e. to ensure a uniform phase modulation, the *i-PMU* is mounted on a Peltier element.

B. EXPERIMENTAL EVALUATION OF THE i-PMU

The experimental setup to evaluate the functionality of the *i-PMU* is shown in Fig. 2 (a). The *i-PMU*'s input fibers are

connected to two external cavity lasers (ECL, 81960A and 81682A from Agilent). While one laser is fixed at $\lambda_1 = 1540$ nm, the second laser (81682A) sweeps with 10 nm/s towards higher wavelength to generate difference frequencies between 50 GHz and 5 THz. Two erbium-doped fiber amplifiers (EDFA, GOA-SP184 from BKtel photonics) boost the output signal of the *i-PMU* to feed 30 mW optical beat signal into the Tx and Rx module, respectively [14], [16], [31]. To drive the SOAs and VOAs of the *i-PMU*, current controllers (CC) from a modular testing platform (Pro8000 from Thorlabs) are used. The particular current values are set in a way that both wavelengths contribute the same power to the resulting optical beat signal in each path. The temperature of the *i-PMU* chip is stabilized to approx. 25°C using a temperature controller (TC) from the same modular testing platform. The PM in the Tx path requires approx. 30 mA for a 2π shift. A data acquisition (DAQ) device (NI-DAQmx USB-6356 from National Instruments) drives the phase modulator with a sawtooth voltage from 0.75 V to 2 V with the frequency $f_{\text{mod}} = 20$kHz. Since the analog output of the DAQ only supports up to 5 mA current, an operational amplifier is added between DAQ and *i-PMU* to provide the required current for the PMs. The Tx requires −1.5 V bias and the photodiode produces approx. 10 mA current. A voltage source (B2902A from Keysight) is used to bias the Tx. Tx and Rx modules are mounted in front of parabolic mirrors to focus the terahertz beam onto the receiver after approx. 30 cm ambient air. The Rx output current is amplified by a transimpedance amplifier (TIA, DHPCA-100 from Femto) with 10^6 V/A gain. For data acquisition, the analog-to-digital converter (ADC) of the DAQ samples the detector signal with 1 Msamples/s and a resolution of 16 bit. In parallel, the DAQ receives the trigger signals of the sweeping laser to correlate the detector signal with the actual terahertz frequency. The digital signals are forwarded to a PC to perform software lock-in amplification (LIA). Therefore, the detector signal is multiplied with a synthetic sine and cosine with $f_{\text{mod}} = 20$ kHz to extract amplitude and phase of the received terahertz signal.

Fig. 2 (b) shows the results of the first spectral measurements of the *i-PMU*. The spectra were measured from 50 GHz to 5 THz with a sweep speed of 1.26 THz per second. The spectral resolution is 1.5 GHz and the integration time at each frequency step is 500 μs. The unprocessed spectrum (black line) shows the characteristic water vapor absorption dips in the detected signal up to approx. 2.8 THz. As a reference, vertical lines show the frequencies of water absorption lines over the measurement range (light blue line) taken from the HITRAN database [32]. Beyond 3 THz, the expected spectral roll-off stops. Measuring a noise trace with blocked terahertz signal but active phase modulation (blue line) reveals that the unprocessed spectrum reaches the noise floor at 3 THz. As a reference, the noise is measured with terahertz signal blocked and phase modulation switched off (grey line). The comparison shows that the phase modulation of the emitter path increases the noise

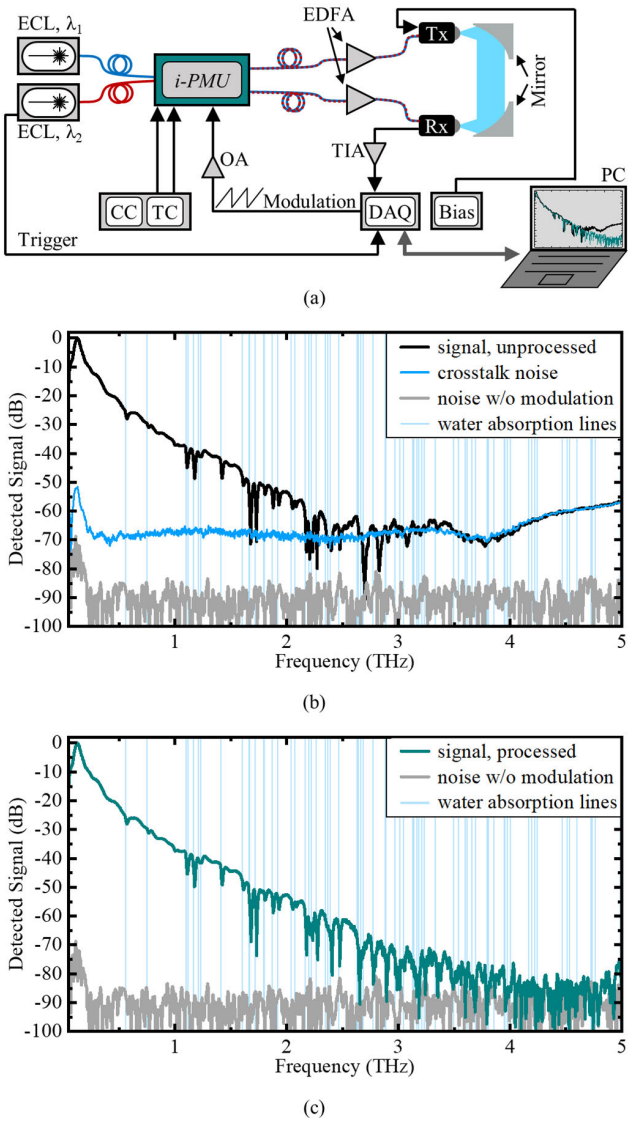

FIGURE 2. (a) Experimental setup for evaluation of the i-PMU. (b) Measured signal from 50 GHz to 5 THz (black line) and noise floor with modulation switched off (grey line). For the unprocessed signal, crosstalk noise (blue line) induced by the modulation limits the spectral bandwidth to 2.8 *THz*. (c) The coherent noise trace is used for subtracting the modulation crosstalk. Hence, the processed spectrum (green line) reaches up to 4 *THz*.

floor of the receiver. This is attributed to thermal crosstalk between Tx phase shifter and Rx waveguides on the InP chip. This results in a modulated photonic LO at the Rx and thus in an increased amplitude after lock-in detection, which masks the actual spectral amplitude. To overcome this, the coherent spectrum of the crosstalk-induced noise is removed from the terahertz spectrum in post-processing. Fig. 2 (c) shows that the processed spectrum (green line) reaches the actual noise floor at 4 THz. Characteristic water vapor lines proof proper spectral measurement up to 4 THz using the *i-PMU*.

Next, the *i-PMU* is directly compared to the fiber-based PMU, which includes a commercial lithium niobate phase

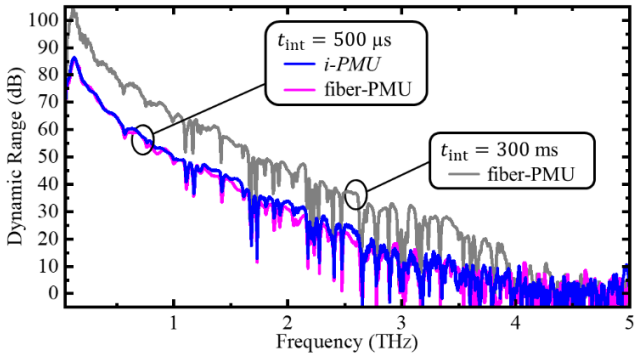

FIGURE 3. Comparison of the conventional, fiber-based PMU and the photonic integrated PMU (i-PMU). In the fast tuning mode, terahertz frequencies from 50 *GHz* to 5 *THz* are swept in <4 s and for short integration times (t_{int} = 0.5 *ms*), the same peak dynamic range of approx. 85 *dB* and maximum terahertz bandwidth of 3.8 *THz* is observed. Using the fiber-based PMU with long integration time (t_{int} = 300 *ms*, total measurement time ≈ 20 *minutes*), the peak dynamic range and terahertz bandwidth increase to 105 *dB* and about 4.5 *THz*, respectively. The instability of the modulation crosstalk prevents longer integration times for the i-PMU.

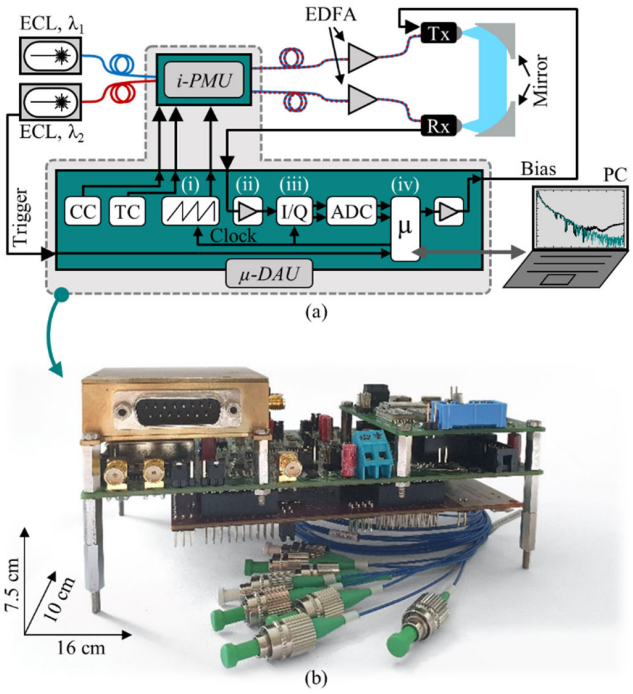

FIGURE 4. (a) Schematic and (b) photograph of the integrated terahertz measurement system including the photonic integrated phase modulation unit (i-PMU) and the electronic driving and acquisition unit (μ-DAU). The electronic unit is based on a microcontroller (μ) and includes a temperature controller (TC), current controller (CC), and analog/digital signal processing.

modulator [26]. For this, the same setup as shown in Fig. 2 (a) is employed and the *i-PMU* is replaced by the fiber-based PMU. The modulation amplitude is adjusted to the PMU, whereas the current and temperature controllers are not used. Fig. 3 shows the direct comparison of the measured dynamic range from 50 GHz to 5 THz. The higher dynamic range is achieved with the fiber-based PMU using an integration time of 300 ms (grey line). Due to the long integration time, the laser cannot be continuously swept, but it needs to be set stepwise to each desired difference frequency. The resulting peak dynamic range is 105 dB and the noise floor is reached at approx. 4.5 THz. However, the measurement time is approx. 20 minutes with this stepped mode. Such a slow measurement cannot be performed with the *i-PMU*, since the measurement of the crosstalk needs to be timely close to the spectral measurement for proper signal processing. For this reason, the *i-PMU* is especially suited for fast measurement with low integration time and fast frequency tuning.

With an integration time of 500 μs and continuous laser frequency tuning, both *i-PMU* and fiber-based PMU can be used for fast coherent spectrum acquisition. Fig. 3 shows spectra from 50 GHz to 5 THz acquired within less than 4 s using the *i-PMU* (blue line) and the fiber-based PMU (magenta line). The peak dynamic range is 85.9 dB and 86.4 dB for the fiber-based PMU and the *i-PMU*, respectively. The bandwidth is approx. 3.9 THz for both. Between 500 GHz and 3 THz, the *i-PMU* enables up to 4.5 dB higher dynamic range. The reason is the different optical attenuation within the PMUs. Unequal attenuation in the optical paths inside the PMUs leads to an unbalanced optical beat signal for Tx and Rx. As a result, the optoelectronic conversion inside the photomixer is less efficient for beat signals with unbalanced optical power for each wavelength [8]. In contrast to the fiber-based PMU, the SOAs and VOAs of the *i-PMU* allow to compensate for individual attenuation of particular paths. Thus the improved beat signal from the *i-PMU* directly improves the photomixing efficiency of Tx and Rx. However, due to the wavelength-dependent gain of the EDFAs, the impact of unbalanced beat signals on the dynamic range is highest around 2 THz.

IV. ELECTRONIC INTEGRATED DRIVING AND ACQUISITION UNIT

A. SYSTEM DESIGN AND CIRCUIT ASSEMBLY

In analogy to the photonic integration of the optical signal processing part, the electronic signal processing is integrated on a printed circuit board (PCB). Therefore, all required functionalities of the previously described lab equipment (Fig. 2 (a)) are realized by commercial integrated circuits (ICs). The system is built around a microcontroller with an evaluation board (LAUNCHXL-F28379D from Texas Instruments), which features all required interfaces to orchestrate the driving and acquisition units. The electronic integrated system is referred to as μ-*DAU*, which stands for *micro*controller-based *d*riving and *a*cquisition *u*nit. Fig. 4 (a) shows the scheme of the μ-*DAU* that replaces the lab equipment. The optical part of the experimental setup is the same as in the previous section including the *i-PMU*. The temperature control is realized using an MDT415T from Thorlabs. Four current controllers (MLD203CLN from Thorlabs) drive the SOAs and VOAs of the *i-PMU*. The values for the

particular driving current and the temperature are set by the microcontroller.

The signal acquisition unit of the μ-*DAU* is divided into four subunits, which are i) generation of the sawtooth signal for the phase modulator, ii) amplification of the detector signal, iii) lock-in amplification of the received signal, and iv) providing the data to an external interface. For subunit (i), a digital-to-analog converter (DAC, AD9102 from Analog Devices) with 14 bit pattern memory serves as a waveform generator to drive the phase modulator. The particular sawtooth pattern and the central clock are given by the microcontroller. To amplify the signal from the Rx (ii), a TIA with fixed gain (10^6 V/A) and a DC block with 100 nF is designed based on an operation amplifier (LTC6268-10 from Analog Devices). Due to the DC block, the minimum modulation frequency is $f_{\mathrm{mod}} = 20$ kHz. For modulation frequencies close to the lower limit, an optional capacitor in the TIA's feedback loop can be used to cut-off high-frequency noise. Subunit (iii) is an integrated I/Q demodulator (AD8333 from Analog Devices), which is used as an LIA to extract I and Q components from the Rx signal. Therefore, the LIA receives the same reference clock as the sawtooth generator. A differential driver (ADA4945-1) converts the single-ended signal from the Rx into a differential signal to feed the I/Q demodulator. The demodulated output signals are filtered by active low-pass filters with a cut-off frequency of $f_c \approx 2$ kHz. In order to fully exploit the analog LIA, two ADCs (AD4022 from Analog Devices) sample I and Q signals with 20 bit resolution depth. Precision ADC drivers (ADA4945-1) allow using the full range of the ADCs if the TIA has maximum output. In subunit (iv) the microcontroller receives the frequency trigger from the sweeping laser and correlates a set of I and Q values with the actual frequency in the terahertz spectrum. These values are provided to an external PC via the USB port on the microcontroller board. Note that in contrast to the lab system, the whole signal processing is performed with analog electronics, i.e. the computational resources for signal acquisition are tremendously reduced.

Finally, an onboard DAC of the microcontroller is used to provide an adjustable bias voltage for the Tx. A subsequent voltage follower based on a simple operation amplifier ensures the required current values for the photodiode of the Tx.

Fig. 4 (b) depicts the stacked PCBs of the μ-*DAU*. The *i-PMU* is mounted in a metallic package on top of the main PCB. Optical fibers allow to access the respective input and output ports of the photonic *i-PMU*. Overall, the whole photonic and electronic integrated system, i.e. *i-PMU* + μ-*DAU*, measures $10 \times 16 \times 7.5$ cm^3.

B. EXPERIMENTAL EVALUATION OF THE μ-DAU

For the characterization of the *i-PMU* in the previous section, the measurement speed of the lab equipment is limited by the analog-digital (A/D) conversion rates of the employed National Instruments data acquisition (DAQ) card and the USB data transfer to the computer for the lock-in signal processing. In order to ensure a continuous data stream from the DAQ to the computer, the maximum trigger rate from the laser results in a trigger scheme with 1.5 GHz spacing. Thus, the frequency resolution is limited to this value for a given laser tuning speed. Due to the integrated signal processing and the higher bit rate of the USB port, the μ-*DAU* can digitize faster trigger signals from the laser simultaneously with the receiver signal. Consequently, the laser tuning speed can be increased to 80 nm/s, resulting in an 8-times faster spectral sweep. Also due to the enhanced data acquisition, the μ-*DAU* can be operated with 25 μs integration time. Thus, the frequency resolution of the μ-*DAU* is 500 MHz, i.e. 3 times lower than the lab system, although the sweep speed is higher. Note that with these settings, the I/Q demodulator operates at 50 kHz, which is close to the lower limit of the IC. The demodulator is originally designed for RF communication and can operate at up to 50 MHz. However, other components, i.e. the lasers and the DAC, prevent even faster measurement. Both can be replaced to further speed up the μ-*DAU*.

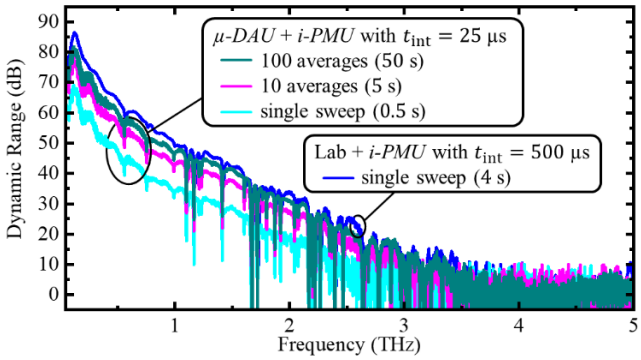

FIGURE 5. Comparison of terahertz spectra acquired with the lab system and the miniaturized system. In both systems, the i-PMU is employed as the PMU. The lab system (blue line) consists of discrete electronic devices and uses digital signal processing. Acquisition of a single terahertz spectrum up to 5 *THz* with 1.5 *GHz* resolution and 500 μs integration time takes 4 *s*. The electronic integrated μ-DAU is based on analog signal processing and can operate at 25 μs integration time. Acquisition of a single frequency sweep with 0.5 *GHz* resolution takes 0.5 *s*. The dynamic range and bandwidth of the μ-DAU increase with the number of averages.

For the evaluation of the electronic integrated μ-*DAU*, spectral measurements are carried out with the lab equipment and the μ-*DAU*. In both cases, the *i-PMU* is employed. Fig. 5 shows spectra from 50 GHz to 5 THz. As a reference, a single spectrum is measured with the maximum ratings of the previously described lab system, i.e. 10 nm/s laser sweep and 500 μs integration time (blue line). For a 5 THz spectrum, a laser tuning of approx. 40 nm is required, which results in 4 s total measurement time for a single sweep. The observed spectral bandwidth is 3.9 THz and the peak dynamic range is 86.4 dB.

Due to the increased tuning speed, a single sweep with the μ-*DAU* takes only 0.5 s. On the other hand, the dynamic range decreases due to the reduced integration time. This leads to

69 dB peak dynamic range and approx. 2.8 THz bandwidth (Fig. 5 light blue line). To improve the spectral quality with the μ-*DAU*, averaging over multiple sweeps reduces the noise and thus increases dynamic range and bandwidth. Accumulating 10 spectral traces results in approx. 9 dB higher dynamic range and enables a bandwidth of approx. 3.4 THz. After averaging over 100 spectra, the peak dynamic range is 81.7 dB and the bandwidth is 3.6 THz. Note, that the pure measuring time of an averaged measurement is the respective multiple of the single sweep time, i.e. 50 s for 100 averages. However, the total duration of an averaged measurement is longer due to a reset time of the external laser after each frequency sweep. Thus, 1s laser downtime is added after each spectrum resulting in 150 s total measurement duration for 100 averages. However, this additional time is solely caused by the employed commercial laser and does not describe the performance of the μ-*DAU*.

Although the spectral performance of the μ-*DAU* is vastly improved by averaging over 100 spectra, further averaging gets more and more inefficient, because of the required timely correlation between spectral trace and crosstalk-induced trace (cf. section III). In future integrated PMUs, the crosstalk between Tx and Rx paths caused by the phase modulators needs to be reduced to further increase the dynamic range. On the electronic site, a lower noise figure is expected from the I/Q demodulator when driven at higher frequencies rather than at the lower edge. Another limitation comes from the USB data rate of the evaluation board of the microcontroller, which is 5 Mbit/s only. The microcontroller itself is feasible to communicate with 480 Mbit/s (USB 2.0). Thus, an optimized PCB would allow for the evaluation of more samples, which can be used to increase the measurement speed or improve lock-in amplification, i.e. higher dynamic range. However, there is a general trade-off between high-speed measurement and dynamic range: The higher the measurement speed, the higher frequencies are required to capture the data. In return, the filters in the signal acquisition chain need to be more broadband. This also leads to an increased noise contribution. Thus, a priori a faster system will always have a higher noise floor. This affects especially analog systems since the filters cannot be adapted to a varying acquisition speed once the PCB is fabricated. In conclusion, the analog system can be further optimized to improve the dynamic range for a certain measurement speed.

V. DISCUSSION

In the previous sections, we demonstrated the functionality of the new photonic integrated *i-PMU* and the electronic integrated μ-*DAU* in combination with measurement parameters specific to our setup (tuning speed, tuning range, frequency resolution, etc.). In this section, we classify our multiple spectrometer configurations as a system relative to other commercial and published cw terahertz spectrometer systems in terms of peak dynamic range and discuss the novelty and potential of our present work.

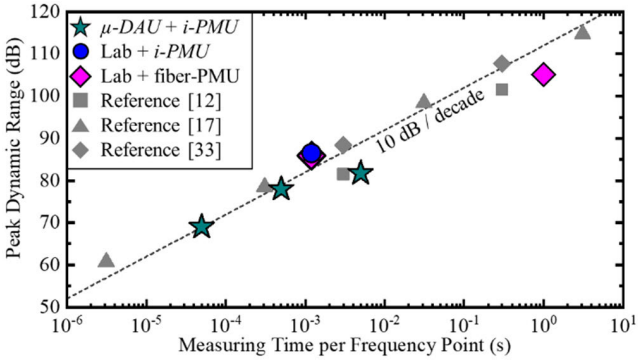

FIGURE 6. Comparison of the peak dynamic range of various spectrometer configurations as a function of the measuring time per frequency point. The actual integration time might be less than the measuring time. A 10 dB increase can be expected for factor 10 in integration time. The dashed line extrapolates this progression for the μ-DAU + i-PMU configuration.

There are fundamental correlations between dynamic range, integration time, measuring speed, and frequency resolution. For example, the noise N is reduced following the square root of integration time $N \propto N_0/\sqrt{t_{\mathrm{int}}}$. This results in a 10 dB increase in dynamic range for a factor of 10 in integration time [17]. That is, increased measuring speed comes at the cost of a reduced dynamic range. For that reason, the share of integration time in the total measuring time should be maximized for an efficient spectrometer. Hence, a fair comparison between spectrometers should consider the dynamic range with respect to the measuring time.

Fig. 6 shows the peak dynamic range achieved with the respective spectrometer configurations as a function of the measuring time per single frequency point. With a 10 dB / decade extrapolation, we can compare the μ-*DAU* + *i-PMU* peak dynamic range with other spectrometer configurations despite varying integration times. This extrapolation reveals that the μ-*DAU* + *i-PMU* configuration has a 4 dB penalty compared to the lab electronics for driving and acquisition. This penalty is attributed to the aforementioned analog electronics, which requires further optimization regarding filter bandwidth for instance.

Fig. 6 also illustrates the impact of timely decorrelation of the reference trace due to thermal crosstalk in the *i-PMU*. The increase in dynamic range is 1.1 dB and 7.3 dB less than expected when averaging 10 and 100 times, respectively. In contrast, without thermal crosstalk in the *i-PMU*, the dynamic range is expected to follow the dashed line in Fig. 6.

As a reference, we compare the μ-*DAU* + *i-PMU* to a commercial terahertz spectrometer [12], [33] and a state-of-the-art prototype system [17]. Note that this only compares the peak dynamic range with respect to the measuring time. The external references employed the same type of Tx and Rx. Thus, the frequency-dependent roll-off can be assumed the same, although the use of different Tx and Rx might result

in a minor offset in the dynamic range. Accordingly, the total spectral bandwidth results from the achieved peak dynamic range and given roll-off, as long as the laser tuning range is sufficient.

From this comparison, we can see that our spectrometer configuration in combination with the used measurement parameters specific to our setup does not provide any new records in terms of available peak dynamic range, measurement speed, terahertz-bandwidth or measurement resolution. Here, we have demonstrated a cw terahertz spectrometer incorporating a dedicated photonic integrated circuit and an electronic driving and acquisition system implemented with commercial microelectronics that aligns well with the performance of commercially available and state-of-the-art scientific cw terahertz spectrometers. This is an important step towards higher levels of integration for cw terahertz spectrometers.

Note that cw terahertz spectrometers using photonic integrated circuits are still the topic of ongoing research. So far, no cw terahertz spectrometer that is fully integrated on a single chip has been presented. Thus, a direct comparison to other cw terahertz spectrometers implemented in photonic integrated circuits is not possible. However, certain functionalities of cw terahertz spectrometer have been photonically integrated and demonstrated as a proof of principle [18], [20], [21], [22], [23], [24]. But they have not been investigated on a system level as discrete spectrometers [4], [5], [6], [13], [17], [26], [27].

For THz system development the presented results are important, since a first photonic integrated device incorporated in a spectrometer opens up a whole range of new possibilities. As a next step, the functionality of a successor design can be extended by integrating fixed frequency and tunable laser sources that are already available on the generic InP foundry [25], [34]. This will reduce the total number of separate components and thus improve the systems footprint and scalability. A future, revised design of the *i-PMU* will also allow us to reduce the on-chip thermal crosstalk by increased spacing between the emitter and receiver paths, especially around the modulator. Furthermore, the development of more efficient components (e.g. lower current for a 2π shift with the modulator) will reduce thermal crosstalk. With this design, we expect the same spectral performance for higher integration times as with the fiber-based PMU.

In a previous publication, we presented a fully fiber-coupled cw terahertz spectrometer employing the same fiber-based PMU and the Lab-DAQ used for evaluation of the *i-PMU* in this work (refer to section III) [27]. Compared to the previously published system, in this work, we use different laser sources and optical amplifiers. This mainly affects the available measurement parameters in terms of available tuning speed, tuning range and frequency resolution. The bottleneck for higher measurement rates and dynamic range per measurement time in both systems is the electronic data acquisition (see section IV and [27]). In section IV, we have demonstrated that our electronic integrated μ-*DAU* can handle 8 times faster laser tuning and 3 times more samples to evaluate (higher frequency resolution) compared to the limitations of the National Instruments DAQ within the parameter range of the lasers we used. This 24 times increased acquisition rate can be transferred to other systems that employ the same style of acquisition scheme, e.g. [27].

With the present work, we are aiming for higher measurement rates by increased laser tuning speed. Please note that the increased data acquisition rate could also be spend for a 24 times increased frequency resolution by maintaining a constant laser tuning speed or even higher frequency resolution by reducing the tuning range or tuning speed. The spectral resolution that can be achieved is ultimately limited by the linewidth and frequency accuracy of the employed laser sources. With the lasers used in this work the minimum frequency step resolution is 12.5 MHz. Furthermore, note that currently, we are only working on the lower end of the capabilities of our peripheral signal processing with the μ-*DAU*. In section IV, we describe multiple options to further increase the measurement rate.

Besides the superior measurement speed, the implementation of analog signal processing tremendously reduces the computational effort. For example, the proposed spectrometer could be extended with multiple emitters and receivers without increased requirements for computing resources. Due to the distributed approach of the proposed system, additional signal processing modules can be added easily. Such a simplified system with multiple sensor heads is advantageous for imaging applications or non-destructive testing at production sites.

VI. SUMMARY

In this paper, we present a miniaturized continuous-wave terahertz spectrometer consisting of a photonic integrated phase modulation unit (*i-PMU*) and a microcontroller-based driving and acquisition unit (μ-*DAU*). With two commercial external lasers as input, the 18 mm^2 sized InP PIC generates a balanced optical beat signal to drive the photoconductive terahertz antennas. To enable fast coherent measurements, the feed for the terahertz Tx is phase modulated. The *i-PMU* is packaged as a fiber-pigtailed device to be compatible with commercial tunable laser sources and state-of-the-art photoconductive antennas. The electronic μ-*DAU* provides all the required drivers to operate the *i-PMU* and features analog signal processing for amplitude and phase acquisition. For the latter, a microcontroller synchronizes the external tunable lasers and drives the phase modulation unit and the signal processing in order to provide the digitized amplitude and phase information as a terahertz spectrum to a PC.

A direct comparison between *i-PMU* and a state-of-the-art fiber-based PMU proved the functionality of the photonic *i-PMU*. Using the same integration time, the *i-PMU* provides even up to 4.5 dB higher dynamic range due to its active

balancing of the two optical tones of the beat signal. For spectral measurements with the *i-PMU* chip, we observe on-chip thermal crosstalk between the modulated Tx path and the Rx path. This crosstalk can be corrected by post-processing using a reference trace. However, since reference and spectrum need to be correlated with respect to time, the dynamic range cannot be improved by increasing the integration time. Despite this limitation, a dynamic range of 86.4 dB and bandwidth of 3.9 THz is achieved using the *i-PMU* with 500 μs integration time. A future, revised design of the *i-PMU* will allow us to reduce the on-chip thermal crosstalk and at the same time further improve the systems footprint and scalability.

To exploit the benefits of miniaturized photonic signal processing, the bulky and expensive lab equipment for driving also needs to be replaced. To this end, we tailored the required driving electronics based on commercial ICs. In addition, the whole signal acquisition is realized on a PCB using analog electronics. The resulting μ*-DAU* for driving and data acquisition is connected via USB and enables 8 times faster spectral measurements with 3 times higher frequency resolution compared to the lab equipment. That is, an acquisition time of only 0.5 s is required for a 5 THz scan with 500 MHz spectral resolution. Here, the measurement speed is limited by the employed tunable laser source. For a single spectral sweep, a terahertz bandwidth of 2.8 THz is achieved and the peak dynamic range is 69 dB. When averaging over 100 traces, for instance, the bandwidth increases to 3.6 THz and the peak dynamic range to 81.7 dB. However, the actual potential of the μ*-DAU* is the high measurement speed required for industrial applications. The μ*-DAU* and *i-PMU* can handle twice the laser sweeping speed, i.e. 5 THz in 0.25 s, keeping the same integration time and resolution. For even higher frequencies, a faster, continuous data stream to the PC would be needed.

The combination of both photonic and electronic integration allows for purpose-specific, miniaturized, and fast terahertz systems. Thus, the demonstrated approach is promising for industry-related applications like non-destructive testing and in-line process control. With averaging, such a system is also suitable for applications in which high dynamic range, high bandwidth, and high frequency resolution are preferable to measurement speed. However, all applications benefit from systems based on standardized and commercially available components, since this leads to more compact systems at lower production costs. Overall, the presented system is an important step toward making optoelectronic cw terahertz spectrometers an affordable and widespread technology in academia and industry.

ACKNOWLEDGMENT

The authors would like to thank Dr. Francisco Soares and HHI's foundry team for fruitful discussions regarding the design of the photonic integrated circuit.

(Simon Nellen and Lauri Schwenson are co-first authors.)

REFERENCES

[1] M. Naftaly, N. Vieweg, and A. Deninger, "Industrial applications of terahertz sensing: State of play," *Sensors*, vol. 19, no. 19, p. 4203, Sep. 2019, doi: 10.3390/s19194203.

[2] S. S. Dhillon, M. S. Vitiello, E. H. Linfield, A. G. Davies, M. C. Hoffmann, J. Booske, C. Paoloni, M. Gensch, P. Weightman, G. P. Williams, and E. Castro-Camus, "The 2017 terahertz science and technology roadmap," *J. Phys. D, Appl. Phys.*, vol. 50, no. 4, Feb. 2017, Art. no. 043001, doi: 10.1088/1361-6463/50/4/043001.

[3] D. M. Mittleman, "Twenty years of terahertz imaging [invited]," *Opt. Exp.*, vol. 26, no. 8, pp. 9417–9431, 2018, doi: 10.1364/oe.26.009417.

[4] N. Vieweg, F. Rettich, A. Deninger, H. Roehle, R. Dietz, T. Göbel, and M. Schell, "Terahertz-time domain spectrometer with 90 dB peak dynamic range," *J. Infr., Millim., Terahertz Waves*, vol. 35, no. 10, pp. 823–832, Oct. 2014, doi: 10.1007/s10762-014-0085-9.

[5] R. J. B. Dietz, N. Vieweg, T. Puppe, A. Zach, B. Globisch, T. Göbel, P. Leisching, and M. Schell, "All fiber-coupled THz-TDS system with kHz measurement rate based on electronically controlled optical sampling," *Opt. Lett.*, vol. 39, no. 22, p. 6482, 2014, doi: 10.1364/ol.39.006482.

[6] T. Yasui, E. Saneyoshi, and T. Araki, "Asynchronous optical sampling terahertz time-domain spectroscopy for ultrahigh spectral resolution and rapid data acquisition," *Appl. Phys. Lett.*, vol. 87, no. 6, pp. 1–4, Aug. 2005, doi: 10.1063/1.2008379.

[7] R. Wilk, T. Hochrein, M. Koch, M. Mei, and R. Holzwarth, "OSCAT: Novel technique for time-resolved experiments without moveable optical delay lines," *J. Infr., Millim., Terahertz Waves*, vol. 32, no. 5, pp. 596–602, May 2011, doi: 10.1007/s10762-010-9670-8.

[8] S. Preu, G. H. Döhler, S. Malzer, L. J. Wang, and A. C. Gossard, "Tunable, continuous-wave terahertz photomixer sources and applications," *J. Appl. Phys.*, vol. 109, no. 6, Mar. 2011, Art. no. 061301, doi: 10.1063/1.3552291.

[9] A. Roggenbuck, H. Schmitz, A. Deninger, I. C. Mayorga, J. Hemberger, R. Güsten, and M. Grüninger, "Coherent broadband continuous-wave terahertz spectroscopy on solid-state samples," *New J. Phys.*, vol. 12, no. 4, Apr. 2010, Art. no. 043017, doi: 10.1088/1367-2630/12/4/043017.

[10] B. Sartorius, D. Stanze, T. Göbel, D. Schmidt, and M. Schell, "Continuous wave terahertz systems based on 1.5 μm telecom technologies," *J. Infr., Millim., Terahertz Waves*, vol. 33, no. 4, pp. 405–417, Apr. 2012, doi: 10.1007/s10762-011-9849-7.

[11] L. Liebermeister, S. Nellen, R. B. Kohlhaas, S. Lauck, M. Deumer, S. Breuer, M. Schell, and B. Globisch, "Terahertz multilayer thickness measurements: Comparison of optoelectronic time and frequency domain systems," *J. Infr., Millim., Terahertz Waves*, Dec. 2021, Art. no. 0123456789, doi: 10.1007/s10762-021-00831-5.

[12] A. J. Deninger, A. Roggenbuck, S. Schindler, and S. Preu, "2.75 THz tuning with a triple-DFB laser system at 1550 nm and InGaAs photomixers," *J. Infr., Millim., Terahertz Waves*, vol. 36, no. 3, pp. 269–277, Mar. 2015, doi: 10.1007/s10762-014-0125-5.

[13] J. Kutz, L. Liebermeister, N. Vieweg, K. Wenzel, R. Kohlhaas, and M. Naftaly, "A terahertz fast-sweep optoelectronic frequency-domain spectrometer: Calibration, performance tests, and comparison with TDS and FDS," *Appl. Sci.*, vol. 12, no. 16, p. 8257, Aug. 2022, doi: 10.3390/app12168257.

[14] M. Deumer, S. Breuer, R. Kohlhaas, S. Nellen, L. Liebermeister, S. Lauck, M. Schell, and B. Globisch, "Continuous wave terahertz receivers with 4.5 THz bandwidth and 112 dB dynamic range," *Opt. Exp.*, vol. 29, no. 25, p. 41819, Dec. 2021, doi: 10.1364/oe.443098.

[15] C. Hepp, S. Lüttjohann, A. Roggenbuck, A. Deninger, S. Nellen, T. Göbel, M. Jörger, and R. Harig, "A cw-terahertz gas analysis system with ppm detection limits," in *Proc. 41st Int. Conf. Infr., Millim., Terahertz Waves (IRMMW-THz)*, Sep. 2016, pp. 1–2, doi: 10.1109/IRMMW-THz.2016.7758344.

[16] S. Nellen, T. Ishibashi, A. Deninger, R. B. Kohlhaas, L. Liebermeister, M. Schell, and B. Globisch, "Experimental comparison of UTC- and PIN-photodiodes for continuous-wave terahertz generation," *J. Infr., Millim., Terahertz Waves*, vol. 41, no. 4, pp. 343–354, Apr. 2020, doi: 10.1007/s10762-019-00638-5.

[17] L. Liebermeister, S. Nellen, R. B. Kohlhaas, S. Lauck, M. Deumer, S. Breuer, M. Schell, and B. Globisch, "Optoelectronic frequency-modulated continuous-wave terahertz spectroscopy with 4 THz bandwidth," *Nature Commun.*, vol. 12, no. 1, pp. 1–10, Feb. 2021, doi: 10.1038/s41467-021-21260-x.

[18] M. Theurer, T. Göbel, D. Stanze, U. Troppenz, F. Soares, N. Grote, and M. Schell, "Photonic-integrated circuit for continuous-wave THz generation," *Opt. Lett.*, vol. 38, no. 19, pp. 3724–3726, Oct. 2013.

[19] M. Kleinert, D. de Felipe, C. Zawadzki, W. Brinker, J. H. Choi, P. Reinke, M. Happach, S. Nellen, M. Mohrle, H. G. Bach, and N. Keil, "Photonic integrated devices and functions on hybrid polymer platform," *Proc. SPIE*, vol. 10098, Feb. 2017, Art. no. 100981A, doi: 10.1117/12.2256987.

[20] M.-H. Lee, S. Nellen, F. Soares, M. Moehrle, W. Rehbein, M. Baier, B. Globisch, and M. Schell, "Photonic integrated circuit with sampled grating lasers fabricated on a generic foundry platform for broadband terahertz generation," *Opt. Exp.*, vol. 30, no. 12, p. 20149, 2022, doi: 10.1364/oe.454296.

[21] G. Carpintero, S. Hisatake, D. De Felipe, R. Guzman, T. Nagatsuma, and N. Keil, "Photonics-based millimeter and terahertz wave generation using a hybrid integrated dual DBR polymer laser," in *IEEE MTT-S Int. Microw. Symp. Dig.*, 2016, pp. 1–3, doi: 10.1109/MWSYM.2016.7540330.

[22] F. van Dijk, M. Lamponi, M. Chtioui, F. Lelarge, G. Kervella, E. Rouvalis, C. Renaud, M. Fice, and G. Carpintero, "Photonic integrated circuit on InP for millimeter wave generation," *Proc. SPIE*, vol. 8988, Mar. 2014, Art. no. 89880Q, doi: 10.1117/12.2036571.

[23] I. Degli-Eredi, P. An, J. Drasbæk, H. Mohammadhosseini, L. Nielsen, P. Tønning, S. Rommel, I. T. Monroy, and M. J. R. Heck, "Millimeter-wave generation using hybrid silicon photonics," *J. Opt.*, vol. 23, no. 4, Apr. 2021, Art. no. 043001, doi: 10.1088/2040-8986/abc312.

[24] G. Carpintero, K. Balakier, Z. Yang, R. C. Guzmán, A. Corradi, A. Jimenez, G. Kervella, M. J. Fice, M. Lamponi, M. Chitoui, F. van Dijk, C. C. Renaud, A. Wonfor, E. A. J. M. Bente, R. V. Penty, I. H. White, and A. J. Seeds, "Microwave photonic integrated circuits for millimeter-wave wireless communications," *J. Lightw. Technol.*, vol. 32, no. 20, pp. 3495–3501, Oct. 2014, doi: 10.1109/JLT.2014.2321573.

[25] M.-H. Lee, F. Soares, M. Baier, M. Möhrle, W. Rehbein, and M. Schell, "53 nm sampled grating tunable lasers from an InP generic foundry platform," *Proc. SPIE*, vol. 11356, Apr. 2020, Art. no. 1135605, doi: 10.1117/12.2554541.

[26] H. Dyball, "A new phase for THz," *Electron. Lett.*, vol. 47, no. 23, p. 1255, 2011, doi: 10.1049/el.2011.3361.

[27] L. Liebermeister, S. Nellen, R. Kohlhaas, S. Breuer, M. Schell, and B. Globisch, "Ultra-fast, high-bandwidth coherent cw THz spectrometer for non-destructive testing," *J. Infr., Millim., Terahertz Waves*, vol. 40, no. 3, pp. 288–296, Mar. 2019, doi: 10.1007/s10762-018-0563-6.

[28] A. Roggenbuck, K. Thirunavukkuarasu, H. Schmitz, J. Marx, A. Deninger, I. C. Mayorga, R. Güsten, J. Hemberger, and M. Grüninger, "Using a fiber stretcher as a fast phase modulator in a continuous wave terahertz spectrometer," *J. Opt. Soc. Amer. B, Opt. Phys.*, vol. 29, no. 4, p. 614, Apr. 2012, doi: 10.1364/josab.29.000614.

[29] N. Grote, M. Baier, and F. Soares, "Photonic integrated circuits on InP," in *Fibre Optic Communication*, vol. 161. Berlin, Germany: Springer, 2017, pp. 799–840.

[30] M. Smit, X. Leijtens, H. Ambrosius, E. Bente, J. Van der Tol, B. Smalbrugge, T. De Vries, E. J. Geluk, J. Bolk, R. Van Veldhoven, and L. Augustin, "An introduction to InP-based generic integration technology," *Semicond. Sci. Technol.*, vol. 29, no. 8, Jun. 2014, Art. no. 083001, doi: 10.1088/0268-1242/29/8/083001.

[31] S. Nellen, S. Lauck, G. Schwanke, M. Deumer, R. B. Kohlhaas, L. Liebermeister, M. Schell, and B. Globisch, "Radiation pattern of planar optoelectronic antennas for broadband continuous-wave terahertz emission," *Opt. Exp.*, vol. 29, no. 6, pp. 8244–8257, 2021, doi: 10.1364/oe.416844.

[32] *HITRAN Database*, Atomic Mol. Phys. Division, Harvard-Smithsonian Center Astrophys., 2022. [Online]. Available: https://hitran.org/

[33] TOPTICA Photonics AG, *TOPTICA's TeraScan 1550*, 2022. [Online]. Available: https://www.toptica.com/products/terahertz-systems/frequency-domain/terascan

[34] F. M. Soares, M. Baier, T. Gaertner, M. Feyer, M. Möhrle, N. Grote, and M. Schell, "High-performance InP PIC technology development based on a generic photonic integration foundry," in *Proc. Opt. Fiber Commun. Conf. Expo. (OFC)*, Mar. 2018, pp. 1–3, doi: 10.1364/OFC.2018.M3F.3.

SIMON NELLEN received the B.Sc. and M.Sc. degrees in physics from the Technical University of Berlin, Germany, in 2012 and 2015, respectively. He is currently pursuing the Ph.D. degree in physics with the Fraunhofer Institute for Telecommunications, Heinrich Hertz Institute (HHI), Berlin, Germany.

From 2012 to 2015, he was a Student Research Assistant with the Terahertz Sensor Systems Group, Fraunhofer HHI. At this time, he investigated ultrafast photoconductive switches for pulsed terahertz generation and detection for his master's thesis. Afterwards, he joined Fraunhofer HHI as a Research Associate. He is the author of more than 70 publications in peer-reviewed international journals and conference proceedings and two inventions. His research interests include photonic devices for continuous-wave terahertz generation and detection, monolithically integrated antennas and radio frequency structures, sensing and communication at terahertz frequencies, and photonic integrated circuits for those applications.

LAURI SCHWENSON received the B.Sc. and M.Sc. degrees in electrical engineering from the Technical University of Berlin, Germany, in 2017 and 2020, respectively. He is currently pursuing the Ph.D. degree in electrical engineering with the Fraunhofer Institute for Telecommunications, Heinrich Hertz Institute (HHI), Berlin, Germany.

From 2018 to 2020, he was a Student Research Assistant with the Terahertz Sensor and Systems Group, Fraunhofer HHI. At this time, he investigated photonic integrated circuits in continuous-wave terahertz spectrometer for his master's thesis. Afterwards, he joined Fraunhofer HHI as a Research Associate. His research interests include photonic integrated circuits for terahertz generation and detection, and photonic and electronic system design for continuous-wave terahertz metrology.

LARS LIEBERMEISTER received the Ph.D. degree in quantum- and nanophotonics from Ludwig-Maximilians-Universität Munich, Munich, Germany, in 2016. Since 2017, he has been with the Terahertz Sensors and Systems Group, Fraunhofer Institute for Telecommunications, Heinrich Hertz Institute, Berlin, Germany, as the Project Leader and the Deputy Group Leader. His current research interests include integrated terahertz photonics, optoelectronic terahertz systems, and terahertz quantum optics.

MILAN DEUMER received the B.Sc. and M.Sc. degrees in electrical engineering from the Technical University of Berlin, Germany, in 2016 and 2018, respectively. He is currently pursuing the Ph.D. degree with the Fraunhofer Institute for Telecommunications, Heinrich Hertz Institute (HHI), Berlin, Germany.

From 2015 to 2019, he was a Student Research Assistant with the Terahertz Sensor and Systems Group, Fraunhofer HHI. At this time, he worked on the characterization of photonic THz sources and detectors, and investigated further improvements of the photodiode-based THz emitters for his master thesis. Afterwards, he joined the Commonwealth Scientific and Industrial Research Organization (CSIRO), Brisbane, QLD, Australia, as a Visiting Researcher. Here he worked on kinetic energy harvesting for battery less IoT devices. In 2020, he returned to the Terahertz Sensor and Systems Group, Fraunhofer HHI to pursue the Ph.D. degree. His research interests include the development of photoconductive antennas for cw THz detection for spectroscopy and THz communications

SEBASTIAN LAUCK received the B.Sc. and M.Sc. degrees in electrical engineering from the Technical University of Berlin, Germany, in 2017 and 2019, respectively. He is currently a Research Associate with the Fraunhofer Institute for Telecommunications, Heinrich Hertz Institute (HHI), Berlin, Germany.

From 2016 to 2019, he was a Student Research Assistant with the Terahertz Sensors and Systems Group, Fraunhofer HHI. During this time, he investigated photodiode-based antenna structures for photonic integrated terahertz emitter as part of his master's thesis. Afterwards, he joined Fraunhofer HHI as a Research Associate and an Engineer for RF design and packaging of THz devices and photonic modulators and a Designer for photonic integrated circuits. His research interests include photonic devices for continuous-wave terahertz generation and detection, the RF design and optical packaging of monolithically integrated modulators, and the design and simulation of broadband terahertz antennas for sensing and communication.

MARTIN SCHELL (Member, IEEE) received the Diploma degree in physics from RWTH Aachen University, Aachen, Germany, in 1989, and the Dr.rer.nat. degree from the Technical University of Berlin, Germany, in 1993. In 1995, he was Visiting Researcher with The University of Tokyo, Tokyo, Japan. From 1996 to 2000, he was a Management Consultant with the Boston Consulting Group. From 2000 to 2005, he was a Product Line Manager, and then the Head of Production and Procurement with Infineon Fiber Optics, Berlin. He is currently the Director of the Fraunhofer Institute for Telecommunications, Heinrich Hertz Institute, Berlin, and a Professor for optic and optoelectronic integration with the Technical University of Berlin. He was a Board Member of the European Photonics Industry Consortium, from 2015 to 2021. He is currently the Chairman of the Competence Network Optical Technologies Berlin/Brandenburg (OptecBB), a Spokesman of the Berlin-Brandenburg Photonics Cluster, and a member of the Photonics21 Board of Stakeholders.

ROBERT B. KOHLHAAS received the M.Sc. degree in physics and the Ph.D. degree, focusing on photoconductive antennas for pulsed terahertz (THz) generation and detection from the Technical University of Berlin, Germany, in 2016 and 2021, respectively. Thereafter, he joined the Fraunhofer Institute for Telecommunications, Heinrich Hertz Institute (HHI), as a Research Associate and a Project Manager. Since 2022, he has been the Head of the Terahertz Sensors and Systems Group, Fraunhofer HHI. He is the author of more than 50 publications in peer-reviewed journals and conference proceedings. His research interests include optoelectronic THz sources and receivers, THz communication links, photonically integrated THz systems, and ultrafast photoconductive materials grown by molecular beam epitaxy.